Electrothermal Analysis of $In_{0.12}Al_{0.88}N$/GaN HEMTs

Marián Molnár[1,2], Gesualdo Donnarumma[1],Vassil Palankovski[1], Ján Kuzmík[1,3],
Daniel Donoval[2], Jaroslav Kováč[2], and Siegfried Selberherr[*]

[1]Advanced Materials and Device Analysis Group at[*]
[*]Inst. for Microelectronics, Technische Universität Wien, Austria
[2]Inst. of Electronics and Photonics, Slovak University of Technology, Bratislava, Slovakia
[3]Inst. of Electrical Engineering, Slovak Academy of Sciences, Bratislava, Slovakia
e-mail: marian.molnar@stuba.sk, molnar@iue.tuwien.ac.at

InAlN/GaN High Electron Mobility Transistors (HEMTs) are very popular because of their promising electrical and thermal properties. With the innovation of these structures and the development of fabrication processes, there are still many serious issues like current collapse or self-heating effects, which must be addressed. In this work, the DC device behavior is studied both experimentally and by means of two-dimensional hydrodynamic device simulations. Very good agreement between measurements and simulations with Minimos-NT is achieved using the hydrodynamic transport model including self-heating and impact ionization effects.

1. Introduction

GaN-based HEMTs attract strong attention due to their material-related properties, such as wide bandgap, high carrier saturation velocity, thermal conductivity, and breakdown field, which are required for high-temperature, high-power, and high-speed applications [1,2,3]. Applications include micro- and millimeter-wave power amplification [4,5] and power switching [6], where maintaining efficiency at high power is a challenge, and is thought to be limited by parasitic thermal effects [7]. Because of this challenge, electrothermal properties of an appropriate HEMT device are investigated, particularly for high drain voltages when impact ionization effects take place. Two-dimensional hydrodynamic device simulations are performed by Minimos-NT [8,9].

2. Device structure

The investigated HEMT device structure is schematically depicted in Fig.1. The heterostructure is grown by metal-organic vapor phase epitaxy (MOVPE). A 300nm thick AlN layer is grown on the 6H-SiC substrate followed by a 2.5μm GaN buffer layer with a 1nm AlN spacer layer and a 7nm $In_{0.12}Al_{0.88}N$ barrier layer on top. The drain and source contacts are prepared by the evaporation of a Ti/Al/Ni/Au metal stack with subsequent rapid thermal annealing, while the gate contact is formed using Ni/Au metallization. The gate-to-drain and the gate-to-source distances are 4.8μm and 1.6μm, respectively, while the gate length is 1.6μm. All layers are non-intentionally doped. The device width is 400μm and there is no passivation. More details about the device fabrication process are reported in [10].

3. Numerical and physics-based modeling

Two-dimensional numerical simulations are performed employing Minimos-NT. The hydrodynamic transport model [11] is used to compute both the transfer and the output

characteristics. It accounts for the Poisson, electron and hole current continuity and energy balance equations, solved self-consistently. Self-heating effects are accounted for by the lattice heat flow equation. The sum of polarization charges at the AlN interfaces equals the polarization charge at the InAlN/GaN interface [12]. Thus, the AlN/InAlN barrier system is represented by a 8nm thick InAlN in the model. Well-calibrated two-valley electron mobility and bandgap energy models are also implemented in the simulator [13]. For $In_{0.12}Al_{0.88}N$ a bandgap energy E_g = 4.84 eV at room temperature is obtained [14]. Due to the divergence of the polarization fields at the InAlN/GaN heterointerface, a two-dimensional electron gas (2DEG) is formed in the quantum well with a density $n_{2DEG}=2.6\times10^{13}$ cm^{-2}. This value, which also depends on the In content in the InAlN layer, gives the best agreement to measured data [14]. The interface between the GaN buffer layer and the AlN nucleation layer is described by a value of polarization charge $\sigma = -2.5\times10^{11}$ cm^{-2}.

Performing hydrodynamic simulations with self-heating, we introduce a substrate thermal contact (Fig.1). We obtain the best agreement with experimental data by using thermal contact resistance $R_{th}=10^{-3}$Kcm^{-2}/W. This value lumps the thermal resistance of the nucleation layer and the SiC substrate, and possible three-dimensional thermal effects [15]. The R_{th} value nicely coincides with that obtained from optical measurements [16]. A new impact ionization model, based on Monte Carlo simulation results [17], was developed and implemented in Minimos-NT.

4. Experimental results and discussion

I-V measurements were performed using a highly-accurate, fully-automated parameter analyzer Agilent 4155C. As discussed below, a very good agreement between measurements and simulations with Minimos-NT is achieved using the hydrodynamic transport model including self-heating and impact ionization effects.

Fig.2 compares the simulation results with and without the self-heating (SH) effect taken into account. Both simulations are performed using the same set of models and model parameters.

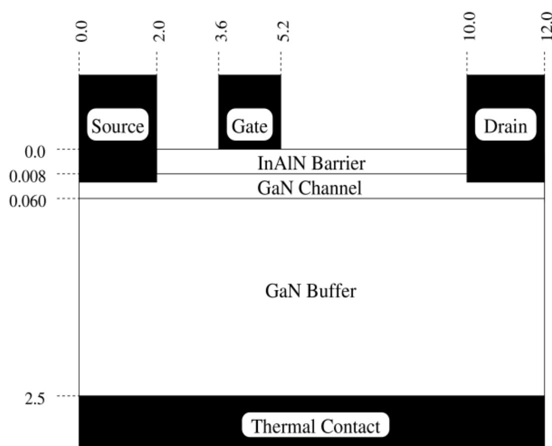

Fig.1 Schematic view of the investigated InAlN/GaN HEMT structure.

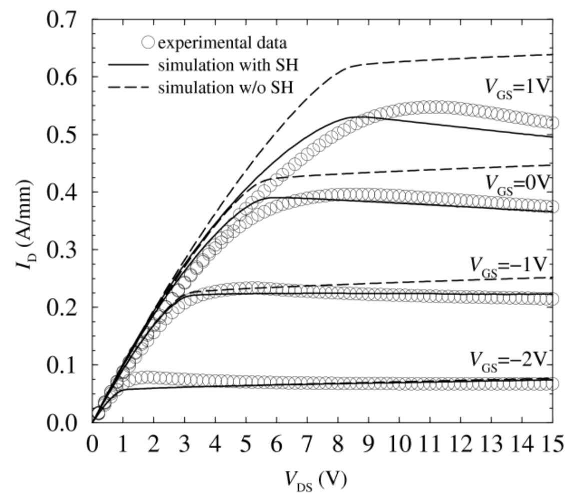

Fig.2 Comparison of measured and simulated output characteristics.

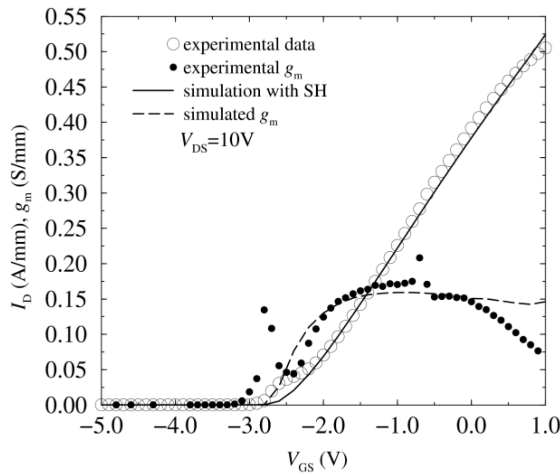

Fig.3 Measured and simulated transfer and transconductance characteristics.

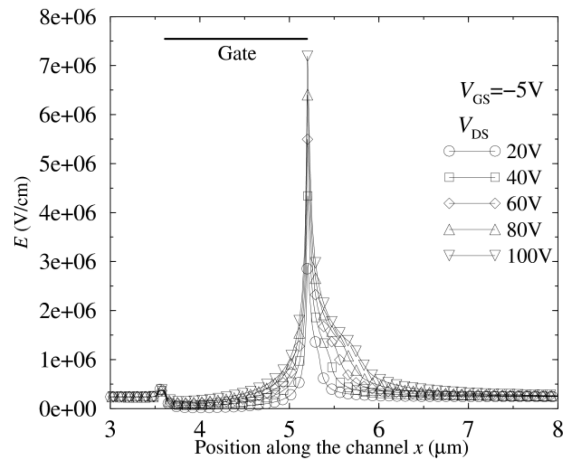

Fig.4 Distribution of electric field E(V/cm) along the channel.

As can be seen in Fig.2, self-heating effects must be included in the model in order to correctly describe the experimentally observed behavior. The influence of self-heating is most pronounced at the device working conditions, where power dissipation culminates, see Fig.2, with a drop in saturated drain current I_D at V_{GS} = 1V as V_{DS} increases.

Fig.3 compares measured and simulated transfer characteristics for a V_{GS} sweep from –5V to 1V at V_{DS} =10V. It also compares the transconductances g_m. The extracted threshold voltage V_{th} is approximately –2.5V. Fig.4 shows the distribution of the electric field E(V/cm) as a function of position along the channel for V_{GS} = –5V and a V_{DS} sweep from 20V to 100V. The maximum of the electric field occurs at the drain side of the gate edge, and reaches approximately 7.2MV/cm at V_{DS} = 100V. Such electric field may be strong enough to trigger the electric breakdown in GaN HEMTs [3].

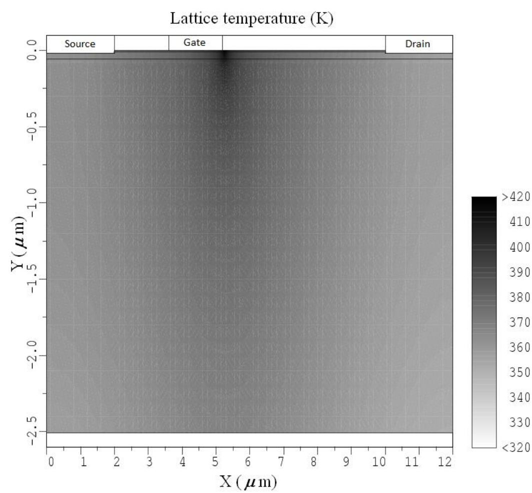

Fig.5 Lattice temperature at V_{GS} = 1V and V_{DS} = 15V.

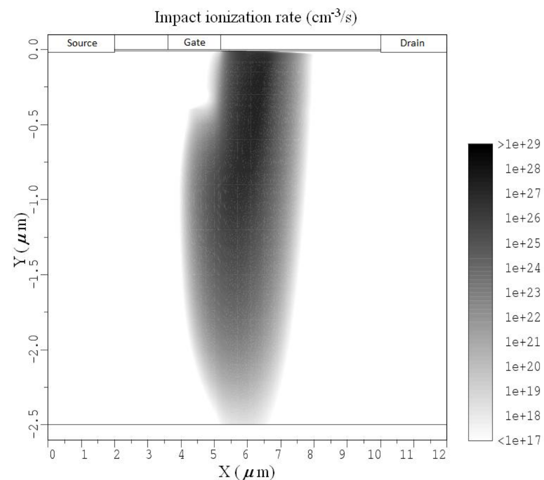

Fig.6 Impact ionization rate at pre-breakdown condition V_{GS} = –5V and V_{DS} = 100V.

Fig.5 shows the distribution of the lattice temperature for V_{GS}=1V and V_{DS}=15V (~8W/mm dissipated power), for which it reaches a maximum of about 420K. Such a moderate temperature increase can be explained by an effective heat sinking through the SiC substrate. Fig.6 shows the impact ionization rate at pre-breakdown condition V_{GS}= –5V and V_{DS} =100V, when the impact ionization rate reaches value up to 10^{29} cm^{-3}/s.

5. Conclusion

Results from electrical measurements and two-dimensional numerical simulations of $In_{0.12}Al_{0.88}N$/GaN HEMTs are presented. Very good agreement between experiment and simulation was obtained for both the transfer and the output characteristics using the hydrodynamic transport model with self-heating and impact ionization models taken into account. Results from the simulation of the HEMT at high temperatures and in the pre-breakdown condition are also presented.

Acknowledgement

This work was supported by the Austrian Science Funds FWF, START Project No.Y247-N13 and by project APVV-0367-11.

References

[1] K. Takahashi, A. Yoshikawa, A. Sandhu, *Wide Bandgap Semiconductors*, Springer, New York, 2007.
[2] S.M. Sze, K.K. Ng, *Physics of Semiconductor Devices*, Wiley, New Jersey, 2007.
[3] R. Quay, *Gallium Nitride Electronics*, Springer, Berlin Heidelberg, 2008.
[4] J.W.Johnson et al., *IEEE Elec.Dev.Lett.*, **25**, 459, 2004.
[5] T. Palacios et al., *IEEE Elec.Dev.Lett.*, **26**, 781, 2005.
[6] W. Saito et al., *IEEE Trans.Elec.Dev.*, **50**, 2528, 2003.
[7] A. Matulionis, in *Proc. Device Research Conference*, Notre Dame, 2004, p.146.
[8] V. Palankovski, R. Quay, *Analysis and Simulation of Heterostructure Devices*, Springer, Wien New York, 2004.
[9] S. Vitanov, *Simulation of High Electron Mobility Transistors*, Dissertation, TU Wien, 2010.
[10] H. Kalisch et al., *J. Crystal Growth*, **316**, 42, 2011.
[11] S. Selberherr, *Analysis and Simulation of Semiconductor Devices,* Springer, Wien New York, 1984.
[12] M. Gonschorek et al., *J.Appl.Phys.*, **103**, 093714, 2008.
[13] S. Vitanov et al., *IEEE Trans.Elec.Dev.*, **59**, 658, 2012.
[14] M. Molnar et al., in *Proc. APCOM'12*, Strbske Pleso, Slovakia, 2012, p.190.
[15] S. Vitanov et al., in *Proc. HETECH'08*, Venice, Italy, 2008, p.159.
[16] J. Kuzmik et al., *J.Appl.Phys.*, **101**, 054508, 2007.
[17] R. Redmer et al., *J.Appl.Phys.*, **87**, 781, 2008.